Early Advanced LIGO binary neutron-star sky localization and parameter estimation

C P L Berry[1], B Farr[2], W M Farr[1], C-J Haster[1], I Mandel[1], H Middleton[1], L P Singer[3], A L Urban[4], A Vecchio[1], S Vitale[5], K Cannon[6], P B Graff[7,8], C Hanna[9,10], S Mohapatra[5,11], C Pankow[4], L R Price[12], T Sidery[1] and J Veitch[1]

[1] School of Physics & Astronomy, University of Birmingham, Birmingham, B15 2TT, UK
[2] Enrico Fermi Institute, University of Chicago, Chicago, IL 60637, USA
[3] Astrophysics Science Division, NASA Goddard Space Flight Center, Greenbelt, MD 20771, USA
[4] Leonard E. Parker Center for Gravitation, Cosmology, and Astrophysics, University of Wisconsin–Milwaukee, Milwaukee, WI 53201, USA
[5] Massachusetts Institute of Technology, 185 Albany St, Cambridge, MA 02139, USA
[6] Canadian Institute for Theoretical Astrophysics, 60 St. George Street, University of Toronto, Toronto, Ontario, M5S 3H8, Canada
[7] Department of Physics, University of Maryland–College Park, College Park, MD 20742, USA
[8] Gravitational Astrophysics Lab, NASA Goddard Space Flight Center, Greenbelt, MD 20771, USA
[9] Perimeter Institute for Theoretical Physics, Ontario, N2L 2Y5, Canada
[10] Pennsylvania State University, University Park, PA 16802, USA
[11] Syracuse University, Syracuse, NY 13244, USA
[12] LIGO Laboratory, California Institute of Technology, Pasadena, CA 91125, USA

E-mail: `cplb@star.sr.bham.ac.uk`

Abstract. 2015 will see the first observations of Advanced LIGO and the start of the gravitational-wave (GW) advanced-detector era. One of the most promising sources for ground-based GW detectors are binary neutron-star (BNS) coalescences. In order to use any detections for astrophysics, we must understand the capabilities of our parameter-estimation analysis. By simulating the GWs from an astrophysically motivated population of BNSs, we examine the accuracy of parameter inferences in the early advanced-detector era. We find that sky location, which is important for electromagnetic follow-up, can be determined rapidly (~ 5 s), but that sky areas may be hundreds of square degrees. The degeneracy between component mass and spin means there is significant uncertainty for measurements of the individual masses and spins; however, the chirp mass is well measured (typically better than 0.1%).

1. Introduction

The advanced generation of ground-based gravitational-wave (GW) detectors, Advanced LIGO (aLIGO) [1] and Advanced Virgo (AdV) [2], begin operation soon: the first observing run (O1) of aLIGO starts in late 2015 [3]. Binary neutron stars (BNSs) are a promising source [4].

Analysis of a signal goes through several stages: detection, low-latency parameter estimation (PE), mid-latency PE and high-latency PE [5]. Each refines our understanding. To discover what we can learn about BNSs, a simulated astrophysically motivated population of BNS signals

(component masses $m_{1,2} \in [1.2, 1.6] M_\odot$, isotropic spins with magnitudes $a_{1,2} \in [0, 0.05]$, and uniformly distributed in volume [6]) has been studied in an end-to-end analysis, with results reported in several publications. Singer *et al.* [6] studied the (low- and mid-latency) prospects for sky localization.[1] Berry *et al.* [7] repeated the analysis using more realistic noise (detector noise from the sixth science run of initial LIGO [8] recoloured to match the expected sensitivity of early aLIGO [9]), in contrast to ideal Gaussian noise. In addition to considering sky localization, Berry *et al.* [7] also investigated measurements of source distance and mass. The latter is influenced by spin, Farr *et al.* [10] completed the high-latency analysis including the effects of spin, considering all aspects of PE. We report results from these studies for O1 PE; further technical details are in the papers themselves.

2. Sky localization

Sky localization can be computed at low-latency by BAYESTAR [11] or at mid- to high-latency by LALINFERENCE [12]. Both are fully Bayesian PE codes; BAYESTAR uses the output of the detection pipeline, while LALINFERENCE matches GW templates to the measured detector strain [13]. Computing templates is computationally expensive; mid-latency PE is done with (non-spinning) TaylorF2 and high-latency PE is done with (fully spin-precessing) SpinTaylorT4. Both are inspiral-only post-Newtonian waveforms [14]. BAYESTAR takes a median time of 4.5 s to calculate the location [11]; the median times for the non-spinning and spinning LALINFERENCE analyses to collect 2000 posterior samples are $\sim 5.7 \times 10^4$ s [7] and $\sim 9.2 \times 10^5$ s [10] respectively.

Despite their differences, BAYESTAR and LALINFERENCE produce consistent results for a two-detector network.[2] The inclusion of spin in PE does not change sky localization for this slowly spinning population (the same may not be true for rapidly spinning black holes). At a constant signal-to-noise ratio (SNR) ϱ, there is also a negligible difference between results from Gaussian and recoloured noise. The scaling of the 50% credible region $\mathrm{CR}_{0.5}$ and 90% credible region $\mathrm{CR}_{0.9}$ with SNR is shown in Fig. 1. Assuming a detection threshold of a false alarm rate of 10^{-2} yr^{-1} ($\varrho \gtrsim$ 10–12), the median $\mathrm{CR}_{0.5}$ ($\mathrm{CR}_{0.9}$) is 170 deg^2 (690 deg^2) using BAYESTAR and 150 deg^2 (630 deg^2) using LALINFERENCE; switching to a threshold of $\varrho \geq 12$ [3], these become 140 deg^2 (520 deg^2) and 120 deg^2 (480 deg^2) respectively [7].

3. Mass and spin

The first estimates for the component masses $m_{1,2}$ come from the detection pipeline, in this case GSTLAL [15]. Full posteriors are constructed by LALINFERENCE. The degeneracy between mass and spin complicates measurements. Excluding spins (as in the mid-latency analysis) means we can miss the true parameter values. Allowing spins to vary over the full (black hole) range of $a_{1,2} \in [0, 1]$ (as in the high-latency analysis) ensures we cover the true value, but potentially means that we consider spin values not found in nature: here, the spins are $a_{1,2} < 0.05$, but we will not know the true distribution in practice.

The chirp mass $\mathcal{M} = (m_1 m_2)^{3/5}/(m_1+m_2)^{1/5}$ is the best measured mass parameter. Fig. 2(a) shows the offset between chirp-mass estimates (maximum likelihood values for GSTLAL and posterior means for LALINFERENCE) and the true values. All methods produce accurate results (offsets $< 0.5\%$) and there is no noticeable difference between recoloured and Gaussian noise. The mid-latency offsets are smaller than the high-latency ones, because our BNSs are slowly spinning (which need not be the case in reality). However, the mid-latency offsets are more statistically significant. The mean values of $(\hat{\mathcal{M}} - \mathcal{M})^2/\sigma^2_{\mathcal{M}}$, where $\sigma_{\mathcal{M}}$ is the posterior standard deviation, are 5.5, 5.1 and 0.7 for the recoloured non-spinning, Gaussian non-spinning and Gaussian spinning analyses respectively. Ignoring spin yields posteriors that are too narrow [7],

[1] Singer *et al.* [6] also considered the second observing run (O2), with AdV joining the network.

[2] This is not the case in a three-detector network if there is not a trigger from all the detectors [6, 11].

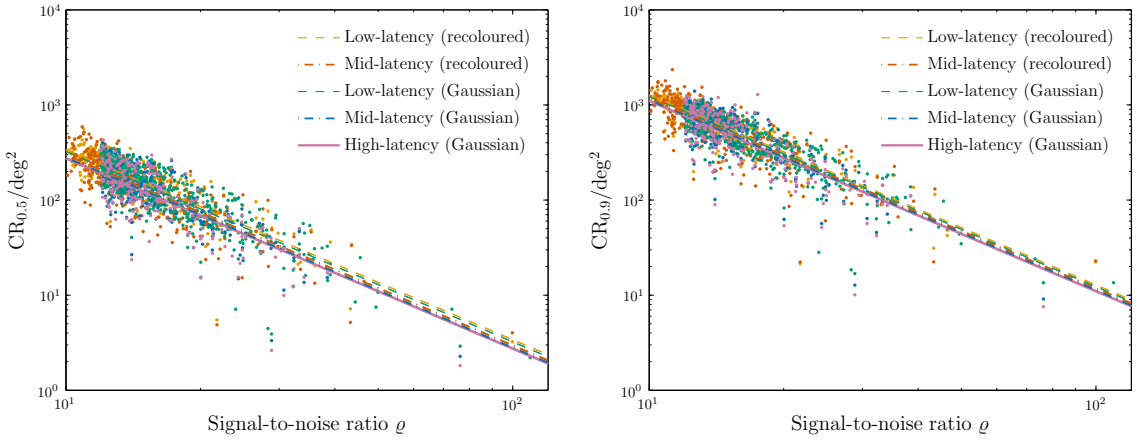

(a) 50% credible region (b) 90% credible region

Figure 1. Sky localization versus SNR for the low-latency BAYESTAR, the mid-latency (non-spinning) LALINFERENCE and the high-latency (spinning) LALINFERENCE analyses [6, 7, 10]. Individual results are indicated by points and lines indicate best fits assuming $\mathrm{CR}_p \propto \varrho^{-2}$; these are $\mathrm{CR}_{0.5} \approx (2.84 \times 10^4)\varrho^{-2}$ deg^2 and $\mathrm{CR}_{0.9} \approx (1.14 \times 10^5)\varrho^{-2}$ deg^2 across the range considered.

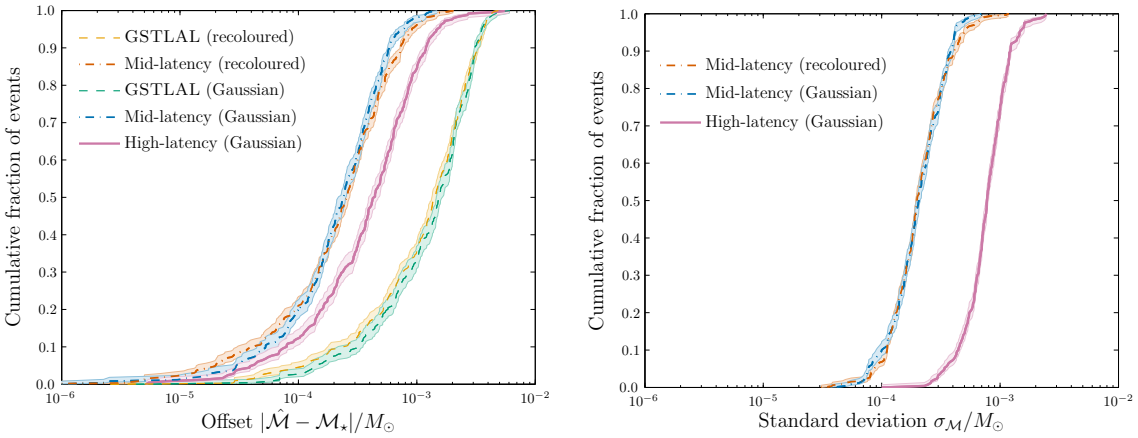

(a) Offset from true value (b) Posterior width

Figure 2. Cumulative fractions of events with (a) offsets in chirp-mass estimates and (b) posterior standard deviations smaller than the abscissa value [7, 10]. The offset is the difference between the true value $\mathcal{M}_*$ and maximum likelihood value from GSTLAL or the posterior mean from (mid- or high-latency) LALINFERENCE. The shaded areas are the 68% confidence intervals on the cumulative distributions.

the distribution of $\sigma_\mathcal{M}$ is shown in Fig. 2(b) [10]; the median values of $\sigma_\mathcal{M}$ are $(2.0 \times 10^{-4})M_\odot$, $(2.1 \times 10^{-4})M_\odot$ and $(7.7 \times 10^{-4})M_\odot$ for the recoloured non-spinning, Gaussian non-spinning and Gaussian spinning analyses respectively.

Measurements of other mass parameters, such as the mass ratio $q = m_2/m_1$ $(0 < q \leq 1)$ or $m_{1,2}$, are less precise, and the degeneracy with spin is more pronounced [10, 13]: the median 50% (90%) credible interval for q is 0.29 (0.59). For our population of low-spin BNSs, the spins are not well measured and have large uncertainties. None of the events have a 50% upper credible bound less than 0.1; the median 50% (90%) upper credible bound is 0.30 (0.70) for a_1 (the

dominant spin) and 0.42 (0.86) for a_2. Low spin values are preferred, but spin magnitudes can only be weakly constrained.

4. Summary

O1 marks the beginning of the advanced-detector era. As time progresses, sensitivities improve and further detectors (AdV, LIGO-India [16] and KAGRA [17]) come online, the prospects for detection and PE will become better [6, 18, 19]. For BNSs, chirp mass is always well measured, but sky localization and spins are more uncertain.

Acknowledgments

This work was supported in part by STFC. This is LIGO document reference LIGO-P1500155. A catalogue of results is available at www.ligo.org/scientists/first2years/.

References

[1] Aasi J *et al.* (LIGO Scientific Collaboration) 2015 *Class. Quantum Grav.* **32** 074001 (*Preprint* 1411.4547)

[2] Acernese F *et al.* (Virgo Collaboration) 2015 *Class. Quantum Grav.* **32** 024001 (*Preprint* 1408.3978)

[3] Aasi J *et al.* (LIGO–Virgo Collaboration) 2013 (*Preprint* 1304.0670v1)

[4] Abadie J *et al.* (LIGO–Virgo Collaboration) 2010 *Class. Quantum Grav.* **27** 173001 (*Preprint* 1003.2480)

[5] Aasi J *et al.* (LIGO–Virgo Collaboration) 2014 The LSC–Virgo White Paper on Gravitational Wave Searches and Astrophysics Tech. Rep. LIGO-T1400054-v7 URL `https://dcc.ligo.org/T1400054/public`

[6] Singer L P *et al.* 2014 *Astrophys. J.* **795** 105 (*Preprint* 1404.5623)

[7] Berry C P L *et al.* 2015 *Astrophys. J.* **804** 114 (*Preprint* 1411.6934)

[8] Aasi J *et al.* (LIGO–Virgo Collaboration) 2015 *Class. Quantum Grav.* **32** 115012 (*Preprint* 1410.7764)

[9] Barsotti L and Fritschel P (LIGO Scientific Collaboration) 2012 Early aligo configurations: example scenarios toward design sensitivity Tech. Rep. LIGO-T1200307-v4 URL `https://dcc.ligo.org/LIGO-T1200307/public`

[10] Farr B *et al.* 2015 (*Preprint* 1508.05336)

[11] Singer L P and Price L R 2015 (*Preprint* 1508.03634)

[12] Veitch J *et al.* 2015 *Phys. Rev. D* **91** 042003 (*Preprint* 1409.7215)

[13] Cutler C and Flanagan E E 1994 *Phys. Rev. D* **49** 2658–2697 (*Preprint* gr-qc/9402014)

[14] Buonanno A, Iyer B, Ochsner E, Pan Y and Sathyaprakash B S 2009 *Phys. Rev. D* **80** 084043 (*Preprint* 0907.0700)

[15] Cannon K *et al.* 2012 *Astrophys. J.* **748** 136 (*Preprint* 1107.2665)

[16] Iyer B, Souradeep T, Unnikrishnan C S, Dhurandhar S, Raja S and Sengupta A (IndIGO Consortium) 2011 LIGO-India LIGO Technical Report M1100296-v2 URL `https://dcc.ligo.org/LIGO-M1100296/public`

[17] Aso Y, Michimura Y, Somiya K, Ando M, Miyakawa O, Sekiguchi T, Tatsumi D and Yamamoto H (KAGRA Collaboration) 2013 *Phys. Rev. D* **88** 043007 (*Preprint* 1306.6747)

[18] Schutz B F 2011 *Class. Quantum Grav.* **28** 125023 (*Preprint* 1102.5421)

[19] Veitch J *et al.* 2012 *Phys. Rev. D* **85** 104045 (*Preprint* 1201.1195)